NANO-INFRARED INVESTIGATION OF THE CM2 CHONDRITE ALH 83100.

J. M. Young[1], T. D. Glotch[1], H. Bechtel[2], S. N. Gilbert Corder[2], and V. E. Hamilton[3], [1]Stony Brook University, 255 Earth and Space Sciences, Stony Brook, NY 11790 (jordan.young@stonybrook.edu), [2]Advanced Light Source - Lawrence Berkeley National Laboratory, Berkeley, CA. [3]Southwest Research Institute, Boulder, CO

Introduction: Mid-infrared (MIR) spectroscopy has been used to great success to quantitatively determine the mineralogy of geologic samples. It has been employed in a variety of contexts from determining bulk composition of powdered samples to spectroscopic imaging of rock thin sections via micro-FTIR. Recent advances allow for IR measurements at the nanoscale, which we have previously used to understand nano-scale compositional variation in ordinary chondrites [1].

Near field infrared (nano-IR) imaging and spectroscopy enable understanding of the spatial relationships between compositionally distinct materials within a sample. This will be of particular use when analyzing returned samples from Bennu and Ryugu. Both asteroids are thought to be compositionally like CI or CM2 carbonaceous chondrites [2], which have undergone considerable aqueous alteration. Returned samples will likely contain olivine/pyroxene chondrules that have been altered into hydrous phyllosilicates, sulfides, carbonates, and other alteration phases [3]. Use of near-field infrared techniques to probe the boundaries between once pristine chondrules and alteration phases at the nanoscale is a novel approach to furthering our understanding of the compositional evolution of carbonaceous asteroids and the processes that drive that evolution.

Furthermore, the use nano-IR imaging and spectroscopy will be an excellent tool for understanding organic molecules found within carbonaceous chondrites and asteroids, including the identity of those compounds and the spatial relationships between organic compounds and mineralogical phases. This information may prove critical to understanding how complex organic compounds found in meteorites formed [4].

Here we report the results of nano-IR spectroscopy and imaging measurements performed on the carbonaceous chondrite Allan Hills (ALH) 83100 (CM2).

Methods: We collected near-field infrared images and spectra of a polished thin-section of the CM2 carbonaceous chondrite ALH 83100 at the Synchrotron Infrared Nano Spectroscopy (SINS) beamline at the Advance Light Source at Lawrence Berkeley National Laboratory. Spectra were collected using a neaspec neaSNOM near-field system coupled with an AFM tip for focusing the synchrotron infrared beam source [5]. Phase and amplitude spectra referenced to a gold standard were collected at harmonics of the AFM tip tapping frequency to remove the far-field signal. The spatial resolution of point spectroscopy measurements is controlled by the radius of curvature of the AFM tip, which is <20 nm. For imaging, we used the same neaspec instrument and a series of tunable lasers (centered at ~6 μm and ~10 μm). Scanned area dimensions were 11 μm x 11 μm. Collected images had dimensions of 550 pixels x 550 pixels, yielding an image resolution of 20 nm/pixel.

Results: Using reflected light microscopy and micro-FTIR image mosaics as guides, we centered our analysis on a chondrule-matrix boundary in ALH 83100. The location of our analysis is shown in Figure 1.

Figure 1. Reflected light image of ALH 83100; Tip of gold arrow shows AFM cantilever position; Red box shows chondrule-matrix boundary where nano-IR measurements were made.

At this location, we generated a series of nano-IR maps using laser wavelengths of 5.97, 6.16, 6.36, 9.25, 9.62, 10.59, and 10.72 μm. Examples of these maps can be seen in Figure 2. These maps show striking spatially distributed compositional variability between the chondrule grain and the surrounding fine-grained matrix. At the 9.62 and 10.72 μm wavelengths, the chondrule grain has lower amplitudes than the surrounding matrix. Interestingly, intra-chondrule and intra-matrix compositional variability was also detected. At the 6.36, 9.62, and 10.59 μm wavelengths there is widespread variability in amplitude within the chondrule grain. Most strikingly is the variability between the chondrule grain in the lower left half of the

maps, and the large triangular grain on the far-right side. The areas are shown by arrows in Figure 2.

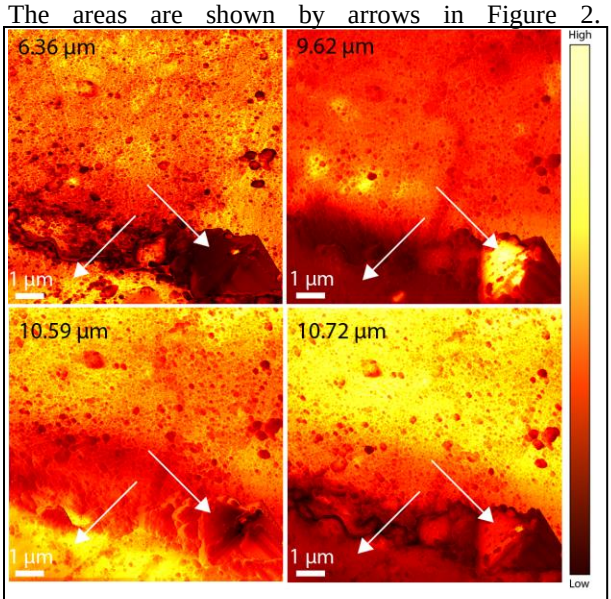

Figure 2. Spectral Images: Yellow pixels represent high amplitude values; Brown-Red pixels represent lower amplitude values Arrows point to spectrally distinct chondrule zones.

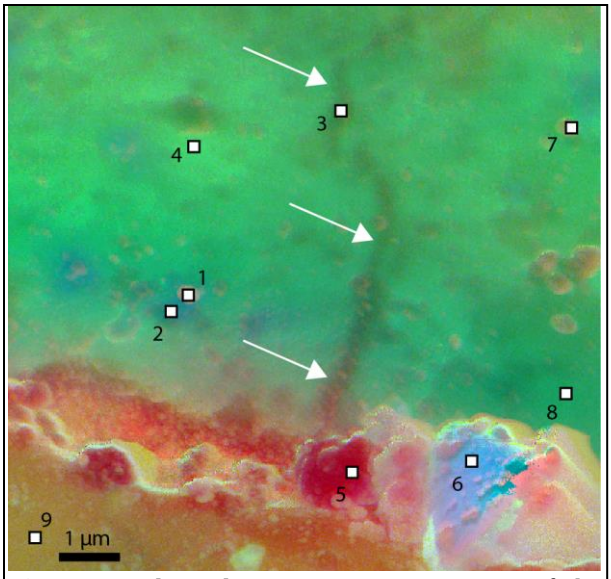

Figure 3. False color RGB image composite of the chondrule-matrix ROI; R, G, and B color channels represent the 10.59, 9.62, and 9.25 µm wavelengths, respectively. Black edged squares represent positions where single spectra were collected. Arrows point to vein-like structure.

Large (0.1 – 0.5 µm) and spectrally distinct clasts appear to exist within the matrix surrounding the chondrule grain and can be seen at all wavelengths. In the 6.36, 10.59, and 10.72 µm wavelengths, spectral variability within the matrix occurs as relatively homogenous zones with small 'web-like' patterns of amplitude contrast dispersed throughout.

Using the map data collected at three discrete wavelengths, we put together a composite false-color image that provides a clearer picture regarding the compositional variability. The composite map, shown in Figure 3, demonstrates which areas of the map are spectrally similar. This map corroborates what was seen in the individual wavelength maps: there is spectral variability within the chondrule grain and the outlying matrix. This map also reveals a long vein like structure that was obscured in the individual wavelength maps.

We also collected spectra at specific locations, which represent various areas of the ROI. The positions from which the point spectra were collected can be seen in Figure 3. We show three of these spectra collected from the various areas on chondrule grain in Figure 4. We see in this plot that the three spectra representing the chondrule grain are distinct. The spectrum of area 6 shows reflectance features at 830, 890, 950, and 970 cm^{-1} respectively. Area 5's spectrum also has a major feature at 970 cm^{-1} and at 1030 cm^{-1} as well. However, it lacks the features the area 6 spectrum has at lower wavenumbers. The spectrum of area 9 has a small reflectance feature at 972 cm^{-1} which it shares with areas 5 and 6 and it has two absorptions at 960 and 985 cm^{-1}. Area 4 represents the surrounding matrix and has a single broad reflectance feature centered ~950 cm^{-1}. These spectra demonstrate clear compositional diversity at micron scales at the chondrule/matrix interface. Spectral interpretation is ongoing.

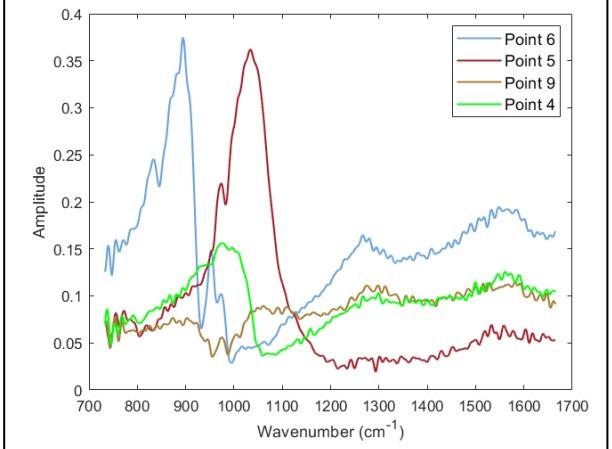

Figure 4. Spectra collected from different areas of interest shown in Figure 3.

References: [1] Glotch T. D. et al. (2019) *NASA ESF* [2] Kitazato K.. et al. (2011) *Science., 364,* 272-275. [3] Hamilton, V.E. et al. (2019) *Nat. Astron 3,* 332-340. [4] Simon, A.A. et al. (2020) *Science, 370.* [5] Amarie S. et al. (2009) *Opt. Express 17,* 21794-21801